

# Size and crystallinity-dependent magnetic properties of $\text{CoFe}_2\text{O}_4$ nanocrystals

C.H. Chia<sup>a,\*</sup>, S. Zakaria<sup>a</sup>, M. Yusoff<sup>a</sup>, S.C. Goh<sup>a</sup>, C.Y. Haw<sup>a</sup>,  
Sh. Ahmadi<sup>a</sup>, N.M. Huang<sup>b</sup>, H.N. Lim<sup>c</sup>

<sup>a</sup>*School of Applied Physics, Faculty of Science and Technology, Universiti Kebangsaan Malaysia, 43600 UKM Bangi, Selangor, Malaysia*

<sup>b</sup>*Solid State Physics Research Laboratory, Physics Department, University of Malaya, 50603 Kuala Lumpur, Malaysia*

<sup>c</sup>*Chemistry Department, Faculty of Science, Universiti Putra Malaysia, 43400 UPM Serdang, Selangor, Malaysia*

Received 17 July 2009; received in revised form 3 August 2009; accepted 23 September 2009

Available online 29 October 2009

## Abstract

$\text{CoFe}_2\text{O}_4$  nanocrystals were synthesized by a wet chemical coprecipitation approach. In order to investigate the effect of degree of crystallinity and mean crystallite size of  $\text{CoFe}_2\text{O}_4$  nanocrystals on the magnetic properties, a series of  $\text{CoFe}_2\text{O}_4$  samples with different degree of crystallinity and mean crystallite size were produced by varying the synthesis and subsequent calcination temperatures. The higher synthesis and subsequent calcination temperatures have resulted in greater degree of crystallinity and bigger mean crystallite size of  $\text{CoFe}_2\text{O}_4$  nanocrystals. The VSM studies showed that the saturation magnetization ( $M_s$ ) and coercivity ( $H_c$ ) of the  $\text{CoFe}_2\text{O}_4$  nanocrystals possessed a linear relationship with the mean crystallite size.

© 2009 Elsevier Ltd and Techna Group S.r.l. All rights reserved.

**Keywords:** A. Powders: chemical preparation; C. Magnetic properties; D. Ferrites; D. Spinels

## 1. Introduction

Nano-sized transition metal oxides with spinel structure have recently received wide attention in several scientific and technological fields [1,2]. Spinel ferrites with cubic unit cell have a formula of  $\text{M}_x\text{Fe}_{3-x}\text{O}_4$ , where the divalent metallic ions ( $\text{M}^{2+}$ ) can be either Fe, Mn, Co, Ni, Cu or Zn. Cobalt ferrite ( $\text{CoFe}_2\text{O}_4$ ), one of the well known hard magnetic materials, has been widely used as high-density recording medium due to its strong magnetic anisotropy, moderate magnetization, and high coercivity at room temperature [3].

There are a number of methods which have been reported previously for the preparation of  $\text{CoFe}_2\text{O}_4$  nanocrystals, including microemulsion [4–6], sol–gel techniques [7], hydrothermal synthesis [8,9], coprecipitation [10–14] and electrochemical synthesis [15]. The chemical coprecipitation is the most widely used method due to its high yield and simplicity in producing ultrafine magnetic nanocrystals. To

date, there are two different chemical coprecipitation methods that have been used to produce  $\text{CoFe}_2\text{O}_4$  nanocrystals, i.e., with and without oxidizing agent. Previous studies reported the precipitation of  $\text{CoFe}_2\text{O}_4$  nanocrystals by mixing  $\text{Fe}^{2+}$ ,  $\text{Co}^{2+}$  and NaOH in the presence of oxidizing agent such as  $\text{H}_2\text{O}_2$  [16] and  $\text{KNO}_3$  [3,17]. The oxidizing agent is required for the formation of  $\text{Fe}^{3+}$  from  $\text{Fe}^{2+}$  as precursor of the formation of  $\text{CoFe}_2\text{O}_4$ . However, the coexistence of  $\text{Fe}^{2+}$  and  $\text{Fe}^{3+}$  ions has resulted in the formation of magnetite ( $\text{Fe}_3\text{O}_4$ ) and  $\text{CoFe}_2\text{O}_4$  which will subsequently affect the purity of the products. In order to avoid this adverse effect, precipitation has been carried out without using oxidizing agent [18,19].

Previous studies have found that the synthesis temperature plays an important role in controlling the size of the  $\text{CoFe}_2\text{O}_4$  which will significantly influence the magnetic properties of the products [11,18]. Besides, a number of attempts have also been made to improve the magnetic properties of the  $\text{CoFe}_2\text{O}_4$  nanocrystals by subsequent calcination of the as-precipitated  $\text{CoFe}_2\text{O}_4$  nanocrystals [16,20,21].

In the present study,  $\text{CoFe}_2\text{O}_4$  nanocrystals are produced using a wet chemical method. The aim of this study is to investigate the effect of crystallite size and degree of crystallinity

\* Corresponding author. Tel.: +60 3 8921 5473; fax: +60 3 8921 3777.

E-mail address: [chia@ukm.my](mailto:chia@ukm.my) (C.H. Chia).

of the  $\text{CoFe}_2\text{O}_4$  nanocrystals on the magnetic properties. A series of  $\text{CoFe}_2\text{O}_4$  nanocrystals with different crystallite size and degree of crystallinity were prepared by varying the synthesis temperature and further calcinations. To the best of our knowledge, these aspects, however, have never been reported altogether in previous studies which are of favorable in controlling the crystallinity and magnetic properties of the  $\text{CoFe}_2\text{O}_4$  nanocrystals.

## 2. Experimental procedures

### 2.1. Materials

Analytical grade of cobalt chloride hexahydrate ( $\text{CoCl}_2 \cdot 6\text{H}_2\text{O}$ ), ferric chloride ( $\text{FeCl}_3$ ) and sodium hydroxide ( $\text{NaOH}$ ) were used without further purification. The solutions of  $\text{Co(II)}$  and  $\text{Fe(III)}$  were prepared by dissolving required weights of  $\text{CoCl}_2 \cdot 6\text{H}_2\text{O}$  and  $\text{FeCl}_3$  in 0.01 M  $\text{HCl}$  separately. This is to avoid any precipitation of iron oxy-hydroxides prior to the synthesis process.

### 2.2. Preparation of $\text{CoFe}_2\text{O}_4$ nanocrystals

In a typical experimental procedure, stoichiometric volume of  $\text{Co}^{2+}$  and  $\text{Fe}^{3+}$  solutions (molar ratio of 1:2) are added into a round bottom flask containing an aqueous solution of  $\text{NaOH}$  at desired temperature. The mixture immediately turned into a dark brown color, indicating the ferrite formation. The mixture is vigorously stirred at a constant stirring rate ( $\sim 200$  rpm) with a turbine mixer and heated at constant temperature for 60 min. The final pH of the suspension is approximately 12. The precipitates are washed with deionized water by the centrifugation at 8000 rpm. The washing and centrifugation are performed 5 times for each precipitate. The obtained precipitate is then dried in an oven at  $50^\circ\text{C}$  for 24 h. The precipitate is then ground into powder for characterization tests. Four samples were produced at different temperatures ( $40$ ,  $60$ ,  $80$  and  $100^\circ\text{C}$ ). In order to produce  $\text{CoFe}_2\text{O}_4$  nanocrystals with greater crystallinity and bigger crystallite size, the as-prepared  $\text{CoFe}_2\text{O}_4$  nanocrystals (precipitated at  $100^\circ\text{C}$ ) are calcined at different temperatures, i.e.,  $300$ ,  $450$ ,  $600$ ,  $750$ ,  $900$  and  $1200^\circ\text{C}$  for 12 h.

### 2.3. Characterizations

All samples are analyzed using a X-ray diffractometry (Siemens diffractometer D5000) with  $\text{Cu K}_\alpha$  radiation

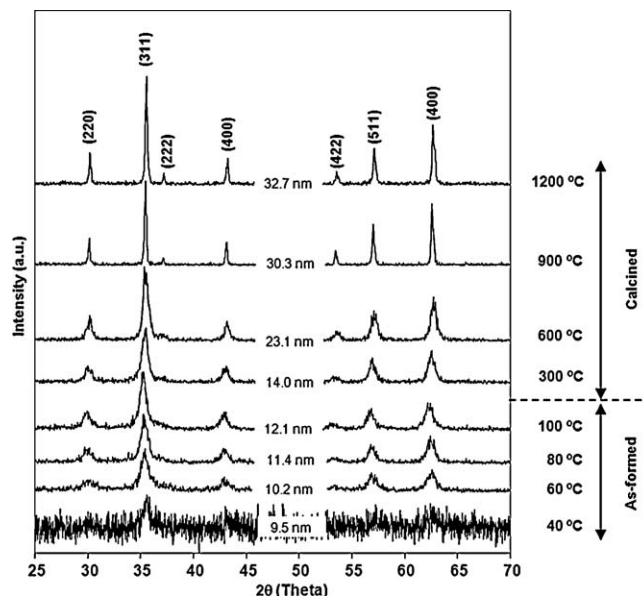


Fig. 1. Size-dependent powder-XRD patterns of as-prepared and calcined  $\text{CoFe}_2\text{O}_4$  nanocrystals produced at different temperatures. The mean crystallite size ( $D_{311}$ ) is estimated by the Scherrer's formula.

( $\lambda = 1.5418 \text{ \AA}$ ). The sample is continuously scanned at a scanning rate of  $0.02^\circ \text{ s}^{-1}$  in the  $2\theta$  range of  $25$ – $80^\circ$ . The mean crystallite size of the crystals is determined by Scherrer's equation [22]

$$D_{hkl} = \frac{0.9\lambda}{\beta \cos \theta} \quad (1)$$

where  $D_{hkl}$  is the average crystallite size,  $\beta$  is the broadening of full width at half maximum intensity (FWHM) of the main intense peak ( $311$ ) in radian,  $\theta$  is the Bragg angle and  $\lambda$  is the radiation wavelength. A transmission electron microscope (Philips CM12) is employed to examine the microstructure and the size of the crystals. The samples are firstly dispersed into the acetone solution (90%) and subjected to an ultrasonic treatment for about 10 min. A drop of the suspension of the crystals is placed on a carbon coated copper grid and then left to dry at the ambient temperature for at least 30 min. The grid is then stored in a desiccator for further tests. The morphology of the crystals and the energy dispersion X-ray analysis (EDX) are studied using a scanning electron microscope (Leo 1450 VP). The magnetic properties are measured at  $25^\circ\text{C}$  using a computerized vibrating sample magnetometer (LDJ 9500).

Table 1  
X-ray diffraction studies and magnetic properties of the produced  $\text{CoFe}_2\text{O}_4$  nanocrystals.

Synthesis temperature ( $^\circ\text{C}$ )	Calcination temperature ( $^\circ\text{C}$ )	$I_{(311)}$ (CPS)	$D_{311}$ (nm)	$M_s$ (emu/g)	$H_c$ (Oe)	$M_r/M_s$
40	–	72	9.5	6.3	53	0.13
60	–	79	10.2	18.7	132	0.14
80	–	89	11.4	32.2	164	0.16
100	–	108	12.1	35.8	249	0.18
100	300	116	14.0	43.2	376	0.25
100	600	148	23.1	54.9	751	0.42
100	900	174	30.3	56.3	1067	0.49
100	1200	228	32.7	60.7	1201	0.39

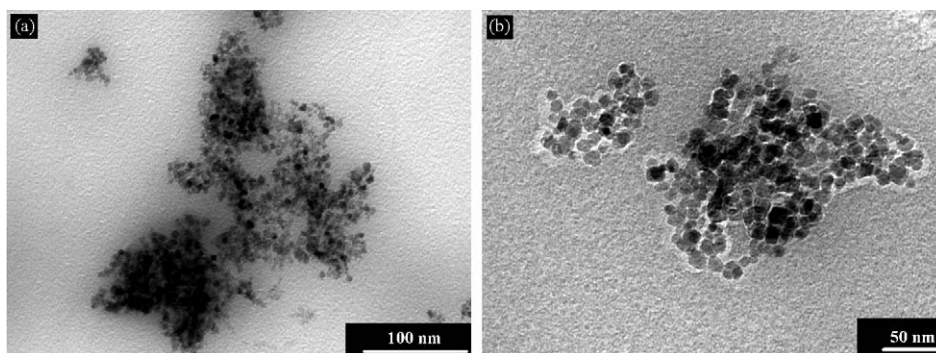


Fig. 2. TEM images of as-prepared  $\text{CoFe}_2\text{O}_4$  nanocrystals synthesized at (a) 40 °C and (b) 100 °C.

### 3. Results and discussion

XRD diffraction patterns of the as-prepared and calcined  $\text{CoFe}_2\text{O}_4$  nanocrystals are presented in Fig. 1. These patterns confirm the formation of cubic spinel type lattice of  $\text{CoFe}_2\text{O}_4$ , which matches well with the standard XRD pattern (JCPDS Card No. 22-1086). No impurities are detected except for the sample produced at 40 °C with the coexistence of amorphous iron oxides ( $\text{FeOOH}$  and  $\alpha\text{-Fe}_2\text{O}_3$ ). The presence of amorphous iron oxides can also be confirmed from the reddish brown color

of the crystals produced at 40 °C. This can probably due to the low temperature has favored the formation of the thermodynamically stable iron oxy-hydroxide phases instead of  $\text{CoFe}_2\text{O}_4$ . Fig. 1 also shows an obvious transition from amorphous to crystal phase as the synthesis temperature increases from 40 to 60 °C and above. The intensity ( $I$ ) of the peaks increases with increasing synthesis temperature from 60 to 100 °C (as shown in Table 1). The mean crystallite size ( $D_{311}$ ) of the  $\text{CoFe}_2\text{O}_4$  nanocrystals increases from  $\sim 9.5$  to  $\sim 12.1$  nm when the synthesis temperature increases from 40 to

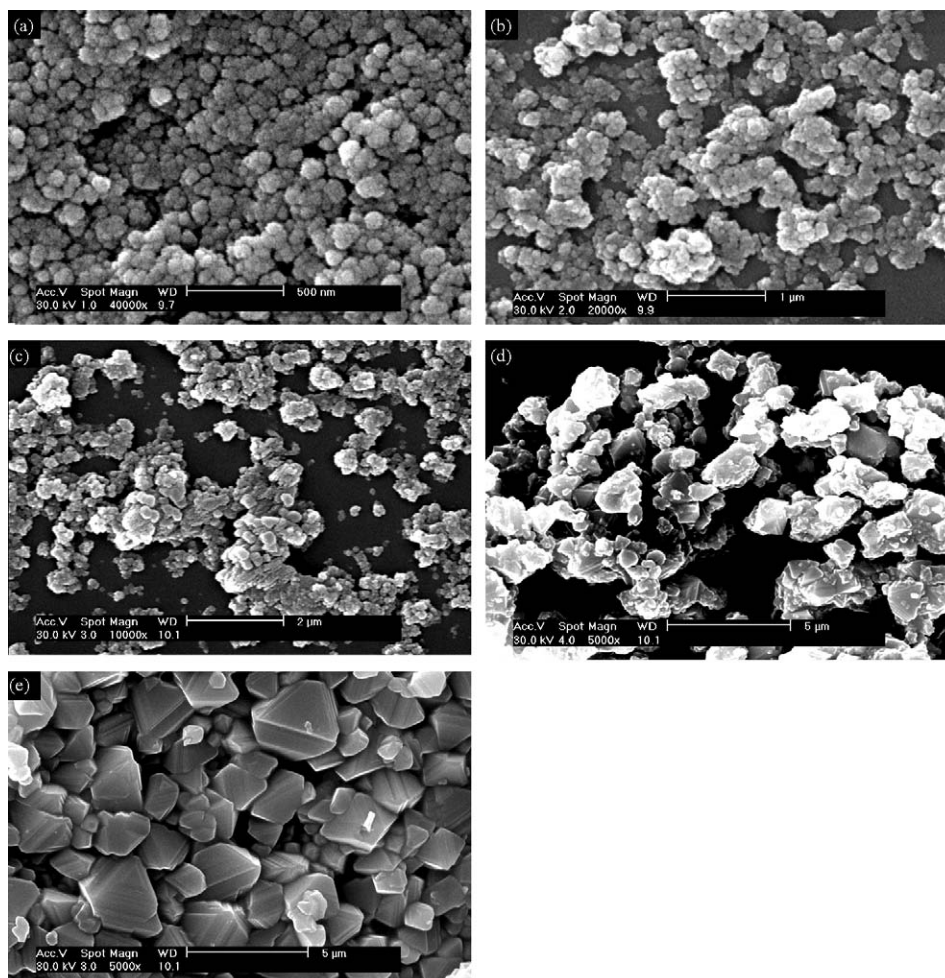


Fig. 3. Atomic ration of Co:Fe of the  $\text{CoFe}_2\text{O}_4$  nanocrystals against calcination temperature.



100 °C. The estimated crystallite size is in accordance with the results from observation under the TEM (Fig. 2), showing that the mean physical size of the  $\text{CoFe}_2\text{O}_4$  nanocrystals is increased from  $\sim 4.9$  to 12.5 nm. This can be attributed to the increase of the rate of crystal growth as a result of expansion of volume and reduction of supersaturation of the system at elevated temperature [23,24]. Moreover, high temperature may enhance the dissolution of amorphous iron oxides, leading to the crystallization of ferrite as  $\text{Co}^{2+}$  ions possess enough energy to diffuse into the ferrite crystal structure [25].

It can be clearly seen that, after the calcination process, the diffraction peaks increases significantly in sharpness and intensity, suggesting the formation of  $\text{CoFe}_2\text{O}_4$  crystals with greater crystallinity and mean crystallite size. The estimated  $D_{311}$  of the  $\text{CoFe}_2\text{O}_4$  nanocrystals increases from 14.0 to 32.7 nm as the calcination temperature increases from 300 to 1200 °C. No appreciable shifts of the diffraction peaks position are detected for all of the calcined samples while the lattice constant ( $a_0$ ) value remains constant ( $\sim 8.398$  Å). In addition, the EDX results (Fig. 3) showed that the atomic ratio of Fe:Co for all of the calcined samples is maintained at  $\sim 2:1$ . These results revealed the sustained spinel structure of the  $\text{CoFe}_2\text{O}_4$  crystals at high calcination temperature.

The morphologies of the as-prepared and calcined  $\text{CoFe}_2\text{O}_4$  nanocrystals are presented in Fig. 4. It can be seen that the as-prepared  $\text{CoFe}_2\text{O}_4$  nanocrystals produced at 100 °C possess clearly defined spherical shape (Fig. 4(a)). The crystals start to associate with one another to form bigger aggregates after calcination at 300 and 600 °C, as shown in Fig. 4(b) and (c), respectively. The crystals are then grown to form bigger crystals at 900 °C and eventually yield cubical structured crystals at 1200 °C. The physical size of the  $\text{CoFe}_2\text{O}_4$  crystals increases with the calcination temperature; however it has resulted in a large size distribution due to the grain growth and densification of the crystals [26]. During the calcination process, solid–vapor surface of the crystals was replaced by solid–solid interface via solid-state diffusion to reduce the overall surface energy.

The  $M$ – $H$  loops of the as-prepared and calcined  $\text{CoFe}_2\text{O}_4$  nanocrystals are presented in Fig. 5. The inset figures show the correlation between the magnetic properties ( $M_s$  and  $H_c$ ) and

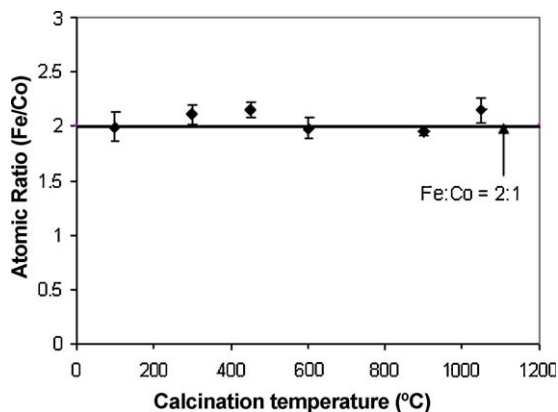


Fig. 4. SEM images of  $\text{CoFe}_2\text{O}_4$  nanocrystals, (a) as-synthesized at 100 °C, (b) calcined at different temperatures, i.e., (b) 300 °C, (c) 600 °C, (d) 900 °C and (e) 1200 °C.

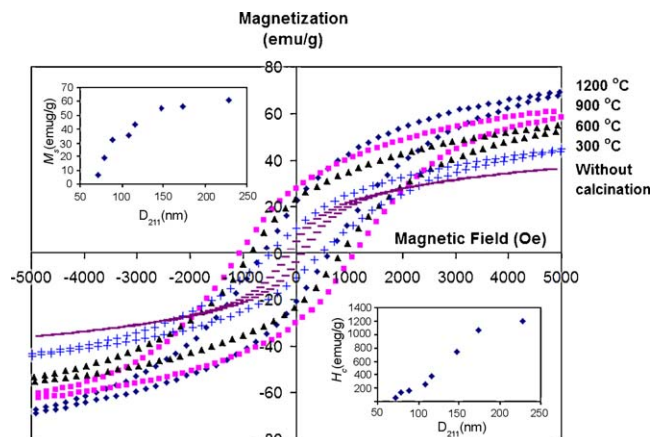


Fig. 5. Magnetization loops of the  $\text{CoFe}_2\text{O}_4$  nanocrystals calcined at different temperatures. The inset figures represent the plots of  $M_s$  and  $H_c$  against mean crystallite size ( $D_{311}$ ).

that of the  $\text{CoFe}_2\text{O}_4$  mean crystallite size. Both  $M_s$  and  $H_c$  of the  $\text{CoFe}_2\text{O}_4$  increased with increasing  $D_{311}$ . This increment is due to the greater degree of crystallinity and lesser effects of inert surface layer of the crystals when the crystals expose to high temperature [27]. In addition, the calcination process has enhanced the rearrangement of distribution of  $\text{Co}^{2+}$  and  $\text{Fe}^{3+}$  ions located in the octahedral and tetrahedral sites. It is also noted that the remanence ratio ( $M_r/M_s$ ) of the crystals increases to 0.49 with the increase of  $D_{311}$  to 30.3 nm and it decreases to 0.39 when the  $D_{311}$  increases to 32.7 nm. This is probably due to the increase of calcination temperature up to 1200 °C has enhanced the exchange coupling interactions of crystals which will affect the magnetization reversal mechanisms [27].

#### 4. Conclusions

In this paper,  $\text{CoFe}_2\text{O}_4$  nanocrystals are produced using chemical coprecipitation method. The degree of crystallinity and mean crystallite size of the  $\text{CoFe}_2\text{O}_4$  nanocrystals are adjusted by varying the synthesis and subsequent calcination temperatures. The higher synthesis and subsequent calcination temperature has resulted in greater degree of crystallinity and bigger mean crystallite size of  $\text{CoFe}_2\text{O}_4$  nanocrystals. The results reveal that the magnetic properties ( $M_s$  and  $H_c$ ) of the  $\text{CoFe}_2\text{O}_4$  nanocrystals have significantly increased with the increase of mean crystallite size.

#### Acknowledgements

The financial support from the Academy of Sciences Malaysia for SAGA grant (STGL-009-2006) is acknowledged. The authors are thankful to Universiti Kebangsaan Malaysia for the facilities and equipments to carry out this study.

#### References

- [1] X.F. Duan, Y. Huang, J.F. Wang, C.M. Lieber, Indium phosphide nanowires as building blocks for nanoscale electronic and optoelectronic devices, *Nature* 409 (2001) 66–69.

- [2] N. Varghese, L.S. Panchakarla, M. Hanapi, A. Govindaraj, C.N.R. Rao, Solvothermal synthesis of nanorods of ZnO, N-doped ZnO and CdO, *Materials Research Bulletin* 42 (2007) 2117–2124.
- [3] C.N. Chinnasamy, M. Senoue, B. Jeyadevam, O. Perales-Perez, K. Shinoda, K. Tohji, Synthesis of size-controlled cobalt ferrite particles with high coercivity and squareness ratio, *Journal of Colloid and Interface Science* 263 (2003) 80–83.
- [4] V. Pillai, D.O. Shah, Synthesis of high-coercivity cobalt ferrite particles using water-in-oil microemulsion, *Journal of Magnetism and Magnetic Materials* 163 (1996) 243–248.
- [5] M. Bonini, A. Wiedenmann, P. Baglioni, Synthesis and characterization of surfactant and silica-coated cobalt ferrite nanoparticles, *Physica A* 339 (2004) 86–91.
- [6] Y.K. Ahn, E.J. Choi, S.H. Kim, H.N. Ok, Magnetization and Mössbauer study of cobalt ferrite particles from nanophase cobalt iron carbonate, *Materials Letters* 50 (2001) 47–52.
- [7] T. Meron, Y. Rosenberg, Y. Lereah, G. Markovich, Synthesis and assembly of high-quality cobalt ferrite nanocrystals prepared by a modified sol–gel technique, *Journal of Magnetism and Magnetic Materials* 292 (2005) 11–16.
- [8] G.B. Ji, S.L. Tang, S.K. Ren, F.M. Zhang, B.X. Gu, Y.W. Du, Simplified synthesis of single-crystalline magnetic  $\text{CoFe}_2\text{O}_4$  nanorods by surfactant-assisted hydrothermal process, *Journal of Crystal Growth* 270 (2004) 156–161.
- [9] N. Millot, S. Le Gallet, D. Aymes, F. Bernard, Y. Grin, Spark plasma sintering of cobalt ferrite nanopowder prepared by coprecipitation and hydrothermal synthesis, *Journal of European Ceramic Society* 27 (2007) 921–926.
- [10] T. Sato, Formation and magnetic properties of ultrafine spinel ferrites, *IEEE Transactions on Magnetics* 6 (1970) 795–799.
- [11] Y.I. Kim, D. Kim, C.S. Lee, Synthesis and characterization of  $\text{CoFe}_2\text{O}_4$  magnetic nanoparticles prepared by temperature-controlled coprecipitation method, *Physica B* 337 (2003) 42–51.
- [12] M.P. Gonzalez-Sandoval, A.M. Beesley, M. Miki-Yoshida, L. Fuentes-Cobas, J.A. Matutes-Aquino, Comparative study of the microstructural and magnetic properties of spinel ferrites obtained by co-precipitation, *Journal of Alloys and Compounds* 369 (2004) 190–194.
- [13] P.C. Morais, V.K. Garg, A.C. Oliveira, L.P. Silva, R.B. Azevedo, A.M.L. Silva, E.C.D. Lima, Synthesis and characterization of size-controlled cobalt-ferrite-based ionic ferrofluids, *Journal of Magnetism and Magnetic Materials* 225 (2001) 37–40.
- [14] B.S. Randhawa, H.S. Dosanjh, M. Kaur, Preparation of spinel ferrites from citrate precursor route—a comparative study, *Ceramic International* 35 (2009) 1045–1049.
- [15] S.D. Sartale, C.D. Lokhande, Electrochemical synthesis of nanocrystalline  $\text{CoFe}_2\text{O}_4$  thin films and their characterization, *Ceramic International* 28 (2002) 467–477.
- [16] M. Rajendran, R.C. Pullar, A.K. Bhattacharya, D. Das, S.N. Chintalapudi, C.K. Majumdar, Magnetic properties of nanocrystalline  $\text{CoFe}_2\text{O}_4$  powder prepared at room temperature: variation with crystallite size, *Journal of Magnetism and Magnetic Materials* 232 (2001) 71–83.
- [17] H. Tamura, E. Matijević, Precipitation of cobalt ferrite, *Journal of Colloid and Interface Science* 90 (1982) 100–109.
- [18] Y. Qu, H. Yang, N. Yang, Y. Fan, H. Zhu, G. Zou, The effect of reaction temperature on the particle size, structure and magnetic properties of coprecipitated  $\text{CoFe}_2\text{O}_4$  nanoparticles, *Materials Letters* 6 (2006) 3548–3552.
- [19] X. Li, C. Kural, Synthesis and characterization of superparamagnetic  $\text{Co}_x\text{Fe}_{3-x}\text{O}_4$  nanoparticles, *Journal of Alloys and Compounds* 349 (2003) 264–268.
- [20] S.M. Montemayor, L.A. García-Cerda, J.R. Torres-Lubián, Preparation and characterization of cobalt ferrite by the polymerized complex method, *Materials Letters* 59 (2005) 1056–1060.
- [21] P.D. Thang, G. Rijnders, D.H.A. Blank, Spinel cobalt ferrite by complexometric synthesis, *Journal of Magnetism and Magnetic Materials* 295 (2005) 251–256.
- [22] Z.B. Huang, F.Q. Tang, Preparation, structure, and magnetic properties of mesoporous magnetite hollow spheres, *Journal of Colloid and Interface Science* 281 (2005) 432–436.
- [23] J. Wang, T. Deng, Y. Dai, Study on the processes and mechanism of the formation of  $\text{Fe}_3\text{O}_4$  at low temperature, *Journal of Alloys and Compounds* 390 (2005) 127–132.
- [24] I.N. Bhattacharya, J.K. Pradhan, P.K. Gochhayat, S.C. Das, Factors controlling precipitation of finer size alumina trihydrate, *International Journal of Mineral Processing* 65 (2002) 109–124.
- [25] J.-P. Jolivet, C. Chanéac, E. Tronc, Iron oxide chemistry, from molecular clusters to extended solid networks, *Chemical Communications* (2004) 481–487.
- [26] J.B. Silva, W.D. Brito, D.S. Mohallem, Influence of heat treatment on cobalt ferrite ceramic powder, *Materials Science and Engineering B* 112 (2004) 182–187.
- [27] W.S. Chiu, S. Radiman, R. Abd-Shukor, M.H. Abdullah, P.S. Khiew, Tunable coercivity of  $\text{CoFe}_2\text{O}_4$  nanoparticles via thermal annealing treatment, *Journal of Alloys and Compounds* 459 (2008) 291–297.